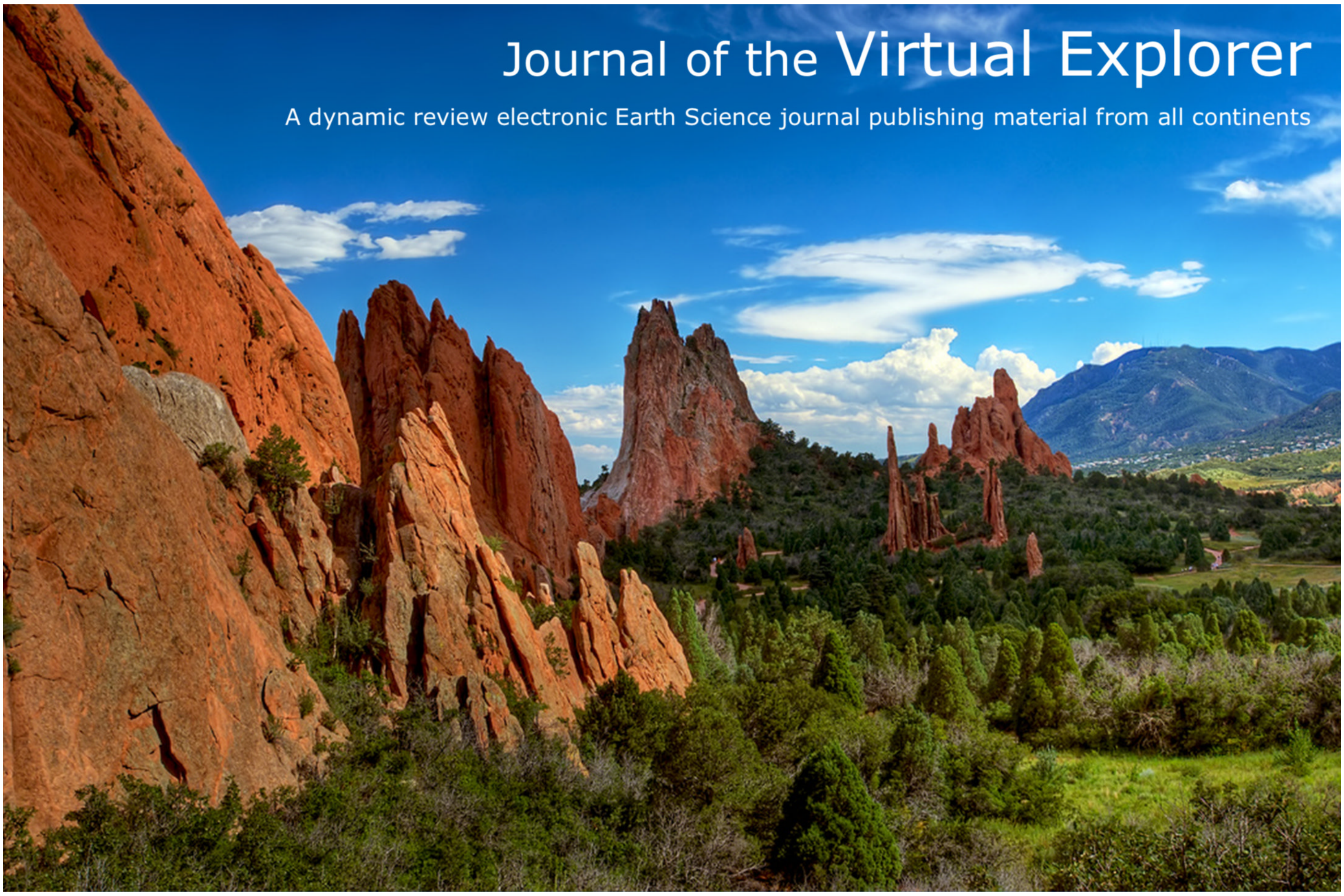

Enhanced Visualization of Seismic Focal Mechanisms and Centroid Moment Tensors Using Solid Models, Surface Bump-outs, and Google Earth

Declan G. De Paor

Journal of the Virtual Explorer, Electronic Edition, ISSN 1441-8142, volume **29**, paper 2
In: (Ed.) Declan De Paor, Google Earth Science, 2008.

Enhanced Visualization of Seismic Focal Mechanisms and Centroid Moment Tensors Using Solid Models, Surface Bump-outs, and Google Earth

Declan G. De Paor

Journal of the Virtual Explorer, Electronic Edition, ISSN 1441-8142, volume **29**, paper 2
In: (Ed.) Declan De Paor, Google Earth Science, 2008.

Abstract: Novel methods for representing earthquake focal mechanisms and centroid moment tensor solutions on virtual globes such as Google Earth™ are introduced. Using solid models and surface bump-outs in conjunction with Keyhole Markup Language (KML), geophysical "beach balls" and other representations of centroid moment tensor solutions may be projected in the Google Earth application so that they appear in the correct orientation at the epicenter location at the source event time. Because the Google Earth virtual globe's surface is opaque, sub-surface data are vertically displaced and a color-coded depth scale is added. The four-dimensional pattern of seismicity in a region may be better understood with the aid of KML's timespan tags which cause data to appear in chronological sequence. Future earthquake and tsunami hazards may be monitored in near-real time on any desktop, laptop, or handheld device that is capable of viewing either the Google Earth virtual globe, or any other KML-savvy virtual globes, such as NASA World Wind.

http://virtualexplorer.com.au/article/2008/195/seismic-model-visualization

Citation: De Paor, D. 2008. Enhanced Visualization of Seismic Focal Mechanisms and Centroid Moment Tensors Using Solid Models, Surface Bump-outs, and Google Earth. In: (Ed.) Declan De Paor, *Journal of the Virtual Explorer*, volume **29**, paper 2, doi: 10.3809/jvirtex.2008.00195

Introduction

Focal mechanism solutions (also known as fault plane solutions) are critical to the evaluation of earthquake hazards and to understanding the spatial and temporal distribution of historic seismicity in relation to local volcanism and global tectonism (McNutt & Sánchez, 2000, Scholz 2002, Stein & Wysession 2002, Lisa, *et al.* 2004). Assuming a simple double-couple motion with no component of displacement normal to the fault plan, a focal mechanism consists of a representation of the orientation of the plane of failure combined with the direction of slip within that plane. Seismic first motion data analysis generally yields two nodal planes, the actual failure plane, and a second "auxiliary" plane oriented perpendicular to the slip vector. Additional factors, including tectonic setting and spatial distribution of seismicity must be considered in order to pick the fault plane and often the ambiguity remains unresolved. Traditionally, focal mechanism are viewed diagrammatically using so-called geophysical beach balls – projections of the focal sphere (Figure 1).

Figure 1. Focal Mechanism Diagram

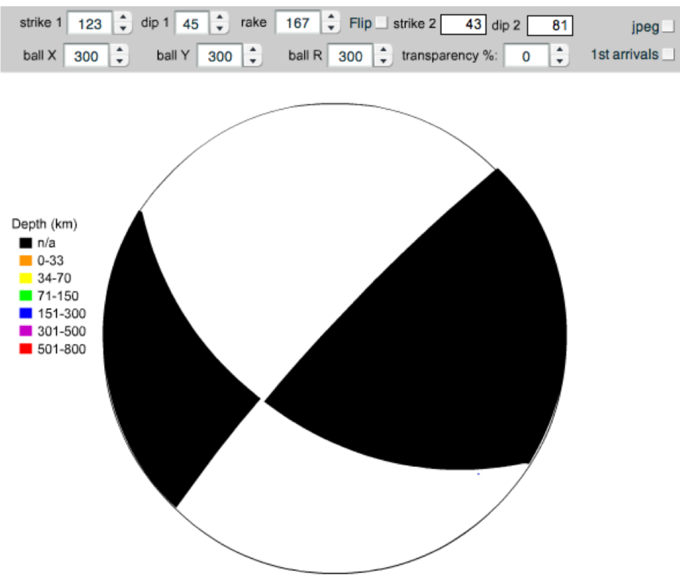

Focal mechanism "beach ball" for an oblique slip fault. Lower hemisphere stereographic projection. Construction is fully discussed in De Paor *et al.* (2006). See also *Glossary* and Cronin (2005).

Geophysical beach balls are lower hemispheric stereographic projections centered on the earthquake hypocenter that show directions of contractional first motions (white) versus dilatational first motions (shaded) separated by two orthogonal great circles representing the two nodal planes. They are constructed based on records from global receiver stations that experience "up" versus "down" first ground motions. Commonly, the radius of the projection is scaled to the earthquake's magnitude and sometimes the shading is colored corresponding to depth. Construction of focal mechanism beach balls is discussed in detail in Cronin (2005) and De Paor *et al.* (2006). We are concerned here with the task of representing focal mechanisms on Google Earth and other virtual globes.

Google Earth™ was chosen over alternative virtual globes such as MS Virtual Earth™, Arc Explorer™, Earth Browser™, *etc.* because it is customizable using Keyhole Markup Language (KML), a dialect of eXtensible Markup Language (XML). The author had been developing structural visualizations using XML-based Tectonic Markup Language (De Paor 1999, Babaie & Babaie 2002) and so conversion to KML was relatively straightforward. NASA World Wind opens KML files but does not yet have a full implementation of all KML version 2.1 features, including solid models. Future development of its open source code may enable the models presented here to be viewed in World Wind.

Building solid models of focal mechanisms

Solid models of geophysical beach balls may be constructed with applications such as 3D Studio Max™, AutoCAD™, Swift3D™, or SketchUp™, among many other 3D drawing and computer-aided design applications. SketchUp benefits from tight integration with Google Earth; for example, while Google Earth is running in the background, the terrain location on which it is currently centered can be imported into SketchUp and conversely, the current SketchUp model can be exported directly to the current Google Earth location.

Generation and manipulation of models in all 3-D modeling programs is tedious and involves a significant learning curve, consequently such applications have not been adopted by the scientific community with the same enthusiasm as Google Earth itself. However, it is not necessary for individual investigators to generate their own models. Instead, existing models such as those presented here can be (i) downloaded and incorporated in Keyhole Markup Archives (KMZ files), (ii) accessed remotely via network links from within KML documents, or most simply, (iii) imported directly into Google Earth using its "Add...Model" menu option.

Figure 2. Models available for download

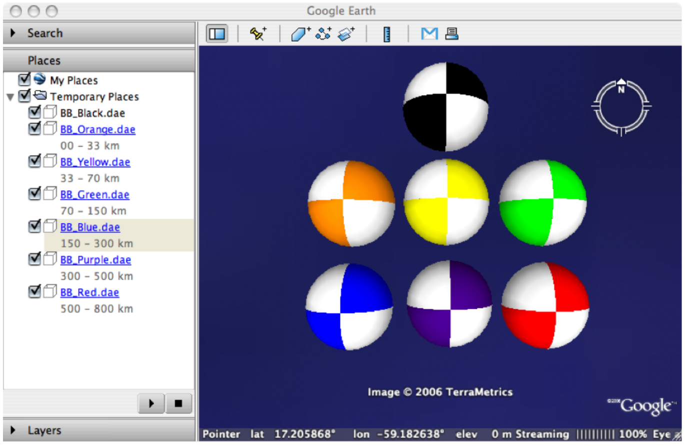

Focal mechanism “beach balls” available for download. Colors can be used to represent depth following the standard USGS depth table (orange <33 km, yellow <70 km, green <150 km, blue 300 km, purple 500 km, red <800 km), or alternatively they can represent event time or other parameters. The black model is used when depth or or data is not implied.

Figure 2 shows a set of beach ball models available for download from the download archive link. They were saved as Collada file types (suffix .dae; see *www.khronos.org*) which can be directly imported into Google Earth. Like KML, Collada files are an XML dialect and their source code can be viewed with any text editor, as shown in Table 1.

Table 1: Sample Collada File Syntax

```
<?xml version="1.0" encoding="utf-8"?>
<COLLADA xmlns="http://www.collada.org/2005/11/COLLADASchema" version="1.4.1">
    <asset>
      <contributor>
        <authoring_tool>Google SketchUp</authoring_tool>
      </contributor>
      <created>2006-12-26T20:21:33Z</created>
      <modified>2006-12-26T20:21:33Z</modified>
      <unit name="meters" meter="1.0"/>
      <up_axis>Z_UP</up_axis>
    ......etc.
```

Colors correspond to the standard USGS depth scale, although they could be used to represent other variables such as event time given an appropriate explanatory legend. The models have a default radius of 1,000 meters, but this may be rescaled from within KML (see below). The default ensures that models are clearly visible on a regional map pattern if moment magnitude is scaled so that Mw = 1.0 corresponds to 1 km, Mw = 2.0 to 2 Km, *etc.*. It is important to bear in mind that solid models viewed from above correspond to upper hemisphere projections, in contrast to traditional lower hemisphere focal mechanism diagrams.

Figure 3a. Semi-transparent ground overlay

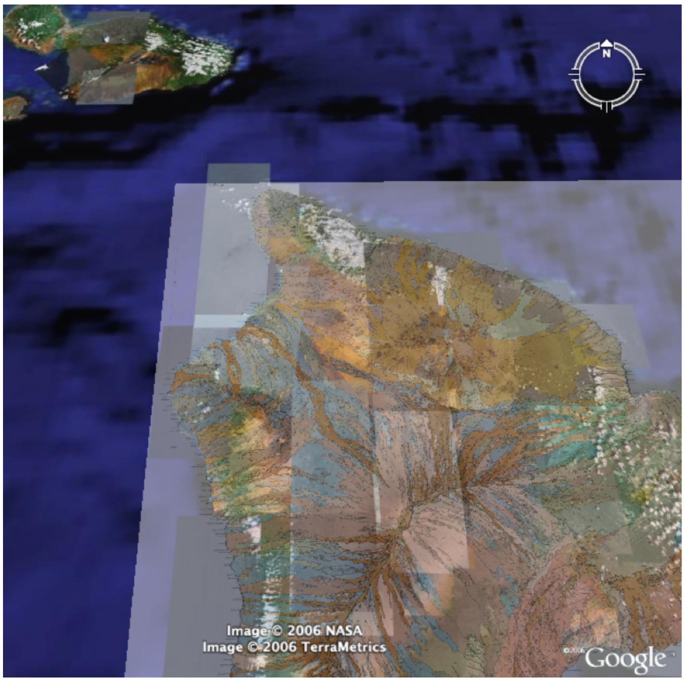

A semi-transparent ground overlay representing the USGS geological map of Hawaii main island. Note that the underlying Google Earth terrain model is opaque.

Figure 3b. Virtual Globe transparency

A virtual globe with opaque continents and fully transparent oceans from *www.mackiev.com*.) Note that the continents other than North and South America are viewed back-to-front, through the interior of the globe. Google Earth currently does not support terrain transparency.

Representing the subsurface in Google Earth

A current limitation of Google Earth is that, whereas models and ground overlays can be made variably transparent, the Google Earth surface itself is always opaque (Figure 3a). Hopefully, future versions of Google Earth will permit sub-surface visualization, a feature which would not be technically difficult to implement. Other virtual globes permit surface transparency – see for example *www.mackiev.com* (Figure 3b). Meanwhile, subsurface data must be "bumped up" by a specified amount. The approach taken here is to include either a depth scale pole (Figure 4a) or a local semi-transparent datum plane ("glass ceiling") that hovers over the local surface to indicate the amount of vertical offset (Figure 4b). Both models can be made visible or invisible, moved to any Lat/Lon location, and bumped out by any specified distance. They are included in the download file. A more labor-intensive approach developed by De Paor & Williams 2006) is to bump-out the terrain, as shown for the main island of Hawaii in Figure 4c. Here, the Google Earth terrain was recorded with screen capture software and projected onto the upper surface of a solid model which was then imported back into Google Earth and positioned precisely over the original terrain. Click here for a movie demonstration [Bump-out Demo].

Figure 4a. Scale pole

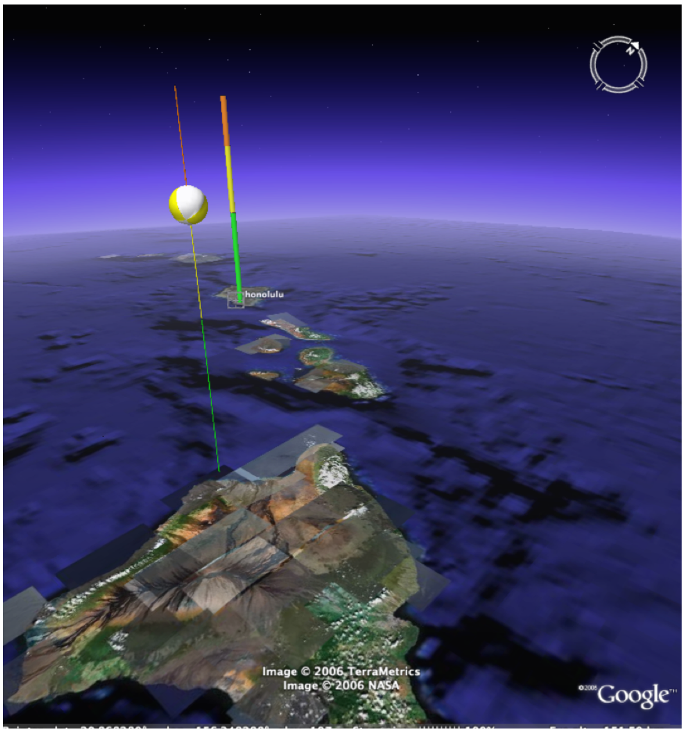

Scale poles indicate the amount of vertical offset using the USGS color chart of Fig. 2.

Figure 4b. "Glass ceiling" reference plane

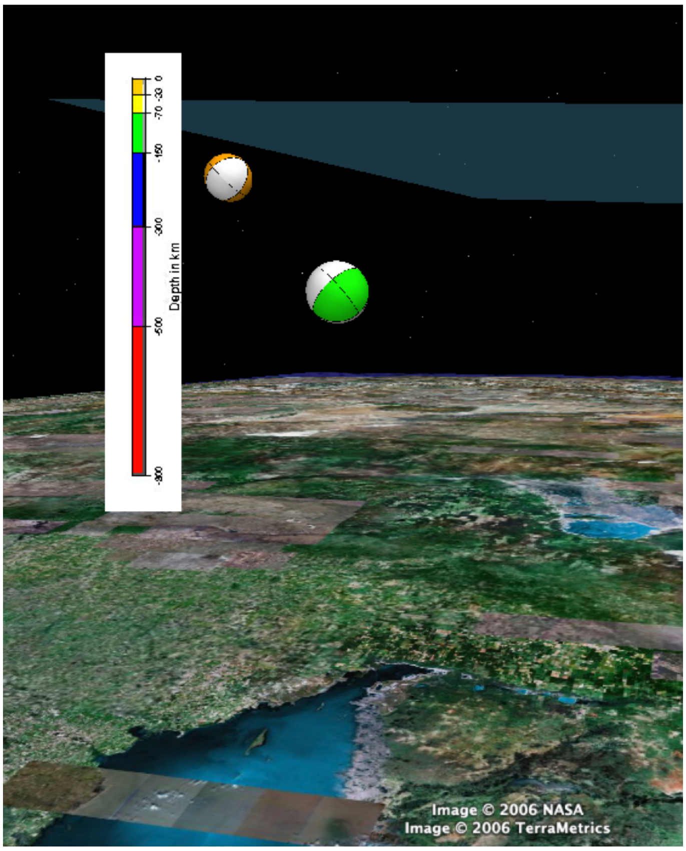

A “glass ceiling” floating over the local region of interest can be used to represent the zero depth datum. Or an image may be imported as a screen overlay.

Figure 4c. Hawaiian surface bumpout

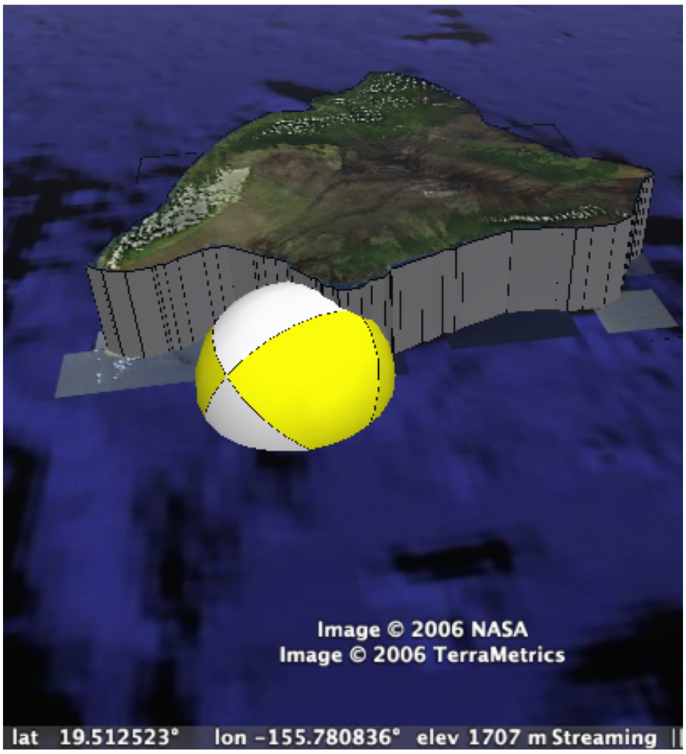

A 50 km high surface bump-out of the Hawaiian main island (here viewed towards the east) was created using SketchUp modeling software. This aids visualization of the 38 km deep Kiholo Bay Earthquake of Oct 2006 (see De Paor & Williams 2006).

Importing focal mechanism models into Google Earth

Geophysical beach balls may be viewed in Google Earth using two methods:

Figure 5. Model location interface

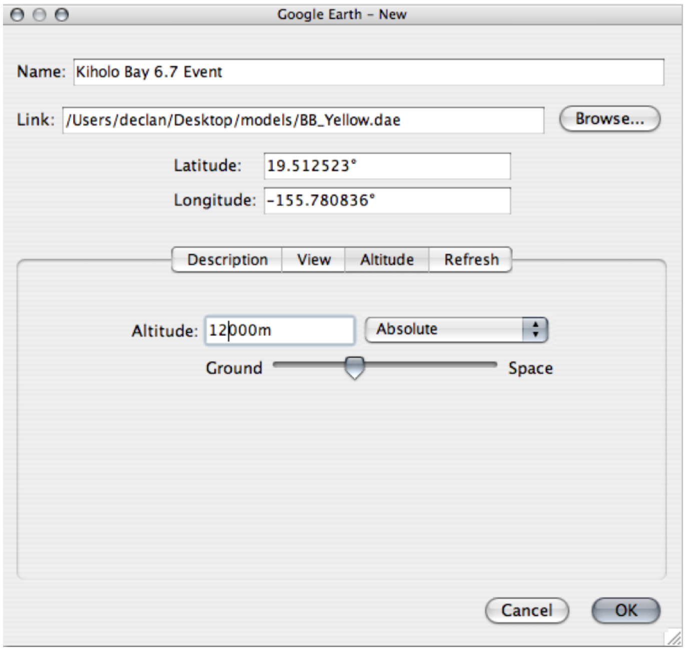

Google Earth interface for adding solid models. The Link field contains the model Collada (.dae) file. Latitude, longitude, and altitude may be specified at import time.

(i) Adding a model directly into Google Earth at run time. As Google Earth is running, a model may be imported using the “Add...model” menu option (Figure 5). The model will first appear at the current geographic location, but its latitude, longitude, and altitude may be edited (see next section).

Figure 6. Default focal mechanism model

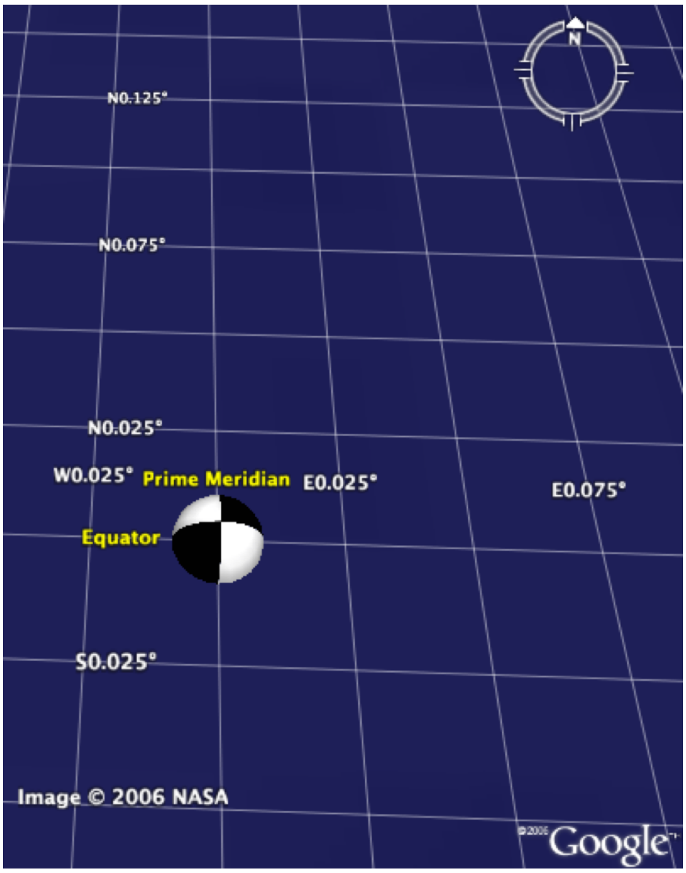

Default position and orientation of the black and white beach ball model. This is generated by the KML code in Table 2.

(ii) Creating and later opening a KML document. The code from Table 2 may be typed into a plain text file using any text editor. The document must be saved with file type “.kml”, e.g., “MyTestFile.kml.” Opening this document with Google Earth reveals the model. If the beach ball models have been downloaded and saved locally in a folder called “models” at the same level as the KML file, then the link text may be shortened to: <href> models/BB_Black.dae </href>. However, in the author’s experience, broken file refs in Google Earth are best avoided by linking only to http URLs.

Table 2: Sample KML File for Accessing a Solid Model

```
<?xml version='1.0' encoding='UTF-8'?>
 <kml xmlns='http://earth.google.com/kml/2.1'>
       <Placemark>
             <Model>
```

```
            <Link>
                <href>http://users.wpi.edu/~declan/models/BB_Black.dae</href>
            </Link>
        </Model>
    </Placemark>
</kml>
```

The 10-line KML file in Table 2 constitutes a complete, working document and is easily understood and adapted to the end user's needs (Numerous textbooks and web sites offering XML tutorials are available, e.g., *www.w3schools.com*. The first line of code identifies the markup language as a version of XML. The XML file structure is based on individual tags identified by angle brackets, case-sensitive text, and pairs of opening and closing tags (the latter identified by the addition of a forward slash). Nested with these tags are the instructions that the reading program uses to render data.

The default location of the model is at zero latitude, zero longitude, and zero altitude (i.e., sea level in the southern Atlantic Ocean west of central Africa). Only the upper hemisphere is visible in Figure 6. The default orientation of the beach ball represents a purely strike slip double couple motion on a vertical fault plane (either sinistral on a NS-striking fault plane or dextral on an EW-striking fault plane). These defaults are changed by writing KML tags as explained below.

Specifying event location and altitude

The location and altitude of a model may be changed using the Google Earth interface of (Figure 5) or by dragging the model's center point in real-time edit mode. However, changes made at run time are not recorded in an existing source KML document. An alternative approach is to open the KML document in a text editor and paste in the code shown in Table 3.

Table 3: Specification of Model Location in KML

```
<?xml version='1.0' encoding='UTF-8'?>
<kml xmlns='http://earth.google.com/kml/2.1'>
    <Placemark>
        <Model>
            <altitudeMode>absolute</altitudeMode>
            <Location>
                <longitude>-156.059</longitude>
                <latitude>19.842</latitude>
                <altitude>1000</altitude>
            </Location>
            <Link>
                <href>http://users.wpi.edu/~declan/mode
            </Link>
        </Model>

    </Placemark>
</kml>
```

After the KML document is saved in the text editor, the version simultaneously open in Google Earth may be "reverted." In the example shown in Figure 7, the altitude value is in meters so the altitude of the beach ball's center is 1 km above sea level.

Figure 7a. Model altitude manipulation

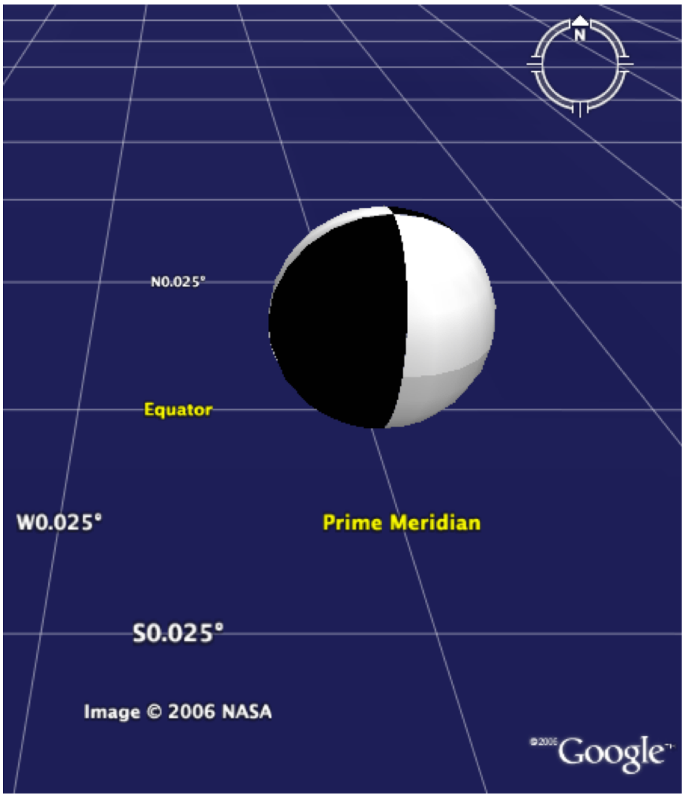

Changing altitude using the KML code in Table 3.

Figure 7b. Model location manipulation

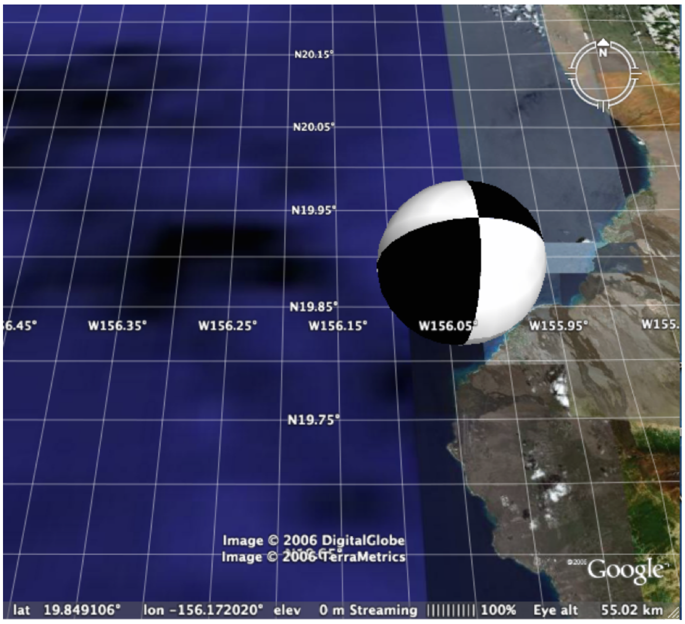

Changing location using the KML code in Table 3

Note that both in the interface of Figure 5 and the code of Table 3, the altitude mode must be chosen as either “absolute” or “relative to ground”. For focal mechanism data, absolute elevation is appropriate.

Representing moment magnitude and orientation

To represent the moment magnitude of an earthquake, it is common to vary the radius of the focal mechanism beach ball. This may be done interactively in Google Earth by dragging model edges in edit mode, but is more accurately achieved in KML using the <Scale> tags as shown in Table 4.

Table 4: Use of Scale Tag to Represent Earthquake Moment Magnitude

```
<?xml version='1.0' encoding='UTF-8'?>
<kml xmlns='http://earth.google.com/kml/2.1'>
      <Location>
         ...
         ...
      </Location>

      <Scale>
           <x>6.7</x>
           <y>6.7</y>
           <z>6.7</z>
      </Scale>
```

```
      <Link>
         ...
         ...
      </Link>
</kml>
```

In the case illustrated, the x, y, and z scaling factors are set to 6.7 to represent an M = 6.7 earthquake. The orientation of the beach ball is critical for interpreting the tectonics setting of the earthquake. USGS NEIC data is reported using three Euler-type angles labeled strike, dip, and slip for each nodal plane. These angles are translated into KML tags <heading>, <roll>, and <tilt> using the system in Table 5.

Table 5: USGS NEIC Stike/Dip/Slip Data and KML

```
<heading> strike </heading>
<roll> dip – 90° </roll>
<tilt> slip </tilt>
```

Figure 8a. 2006 Kurile earthquake

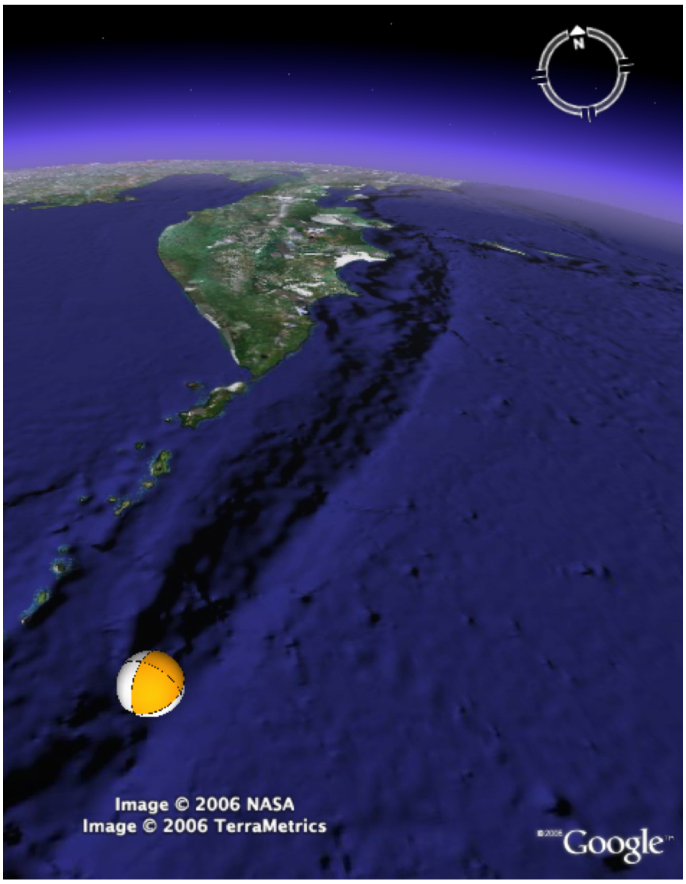

Setting beach ball model orientation. This example shows the 2006 Kurile earthquake without any surface bump-out (altitude = 0). Note that this may be confidently interpreted as a northwest dipping (subduction-zone-parallel) low angle thrust as the depth is too great for a high angle sedimentary slump in the overriding plate.

Figure 8b. Andean data

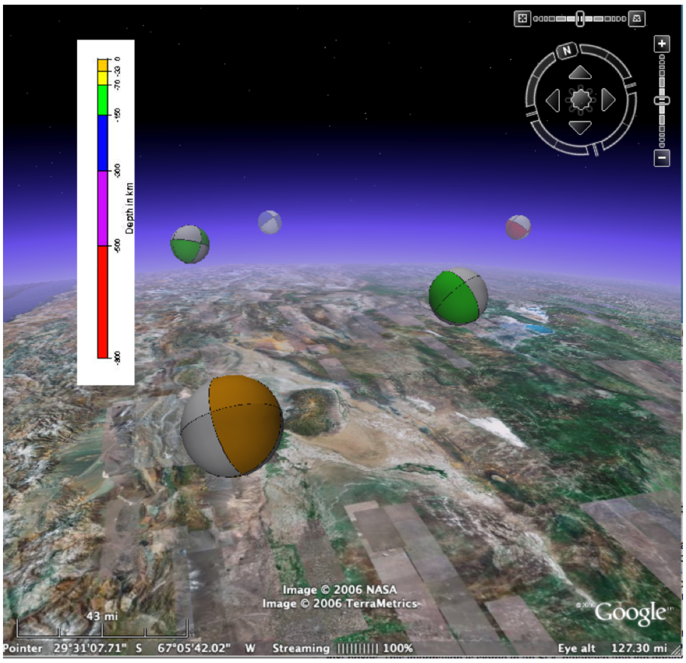

Setting beach ball model orientation. Historic data from the Argentinian Andes (source USGS NEIC).

Adding focal plane solid models

The combination of focal mechanism diagrams and depth data is intended to convey a full three-dimensional understanding of earthquake distributions. However, it is difficult for an observer to determine whether a particular nodal plane is shared by neighboring seismic events or whether a plane's orientation is precisely parallel to an underlying map feature, for example. To aid visualization and analysis, solid models of nodal planes are here added to the beach balls (Figure 9).

Figure 9a. Nodal planes

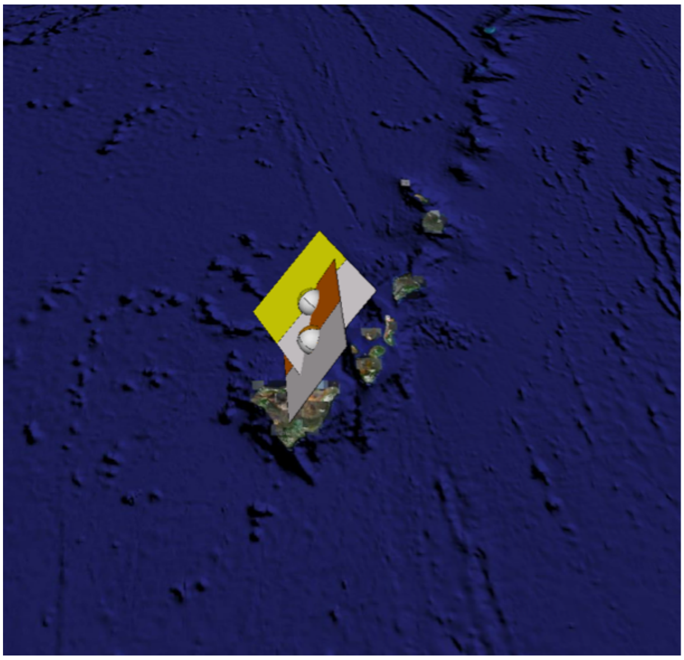

Addition of nodal plane solid models aids visualization of the spatial relationships of neighboring focal mechanisms. It is clear that both hypocenters lie on a common nodal plane.

View of data from the Kiholo Bay event, Hawaii, 2006 (data from USGS NEIC and Havard/LDEO).

Figure 9b. Nodal planes - alternate view

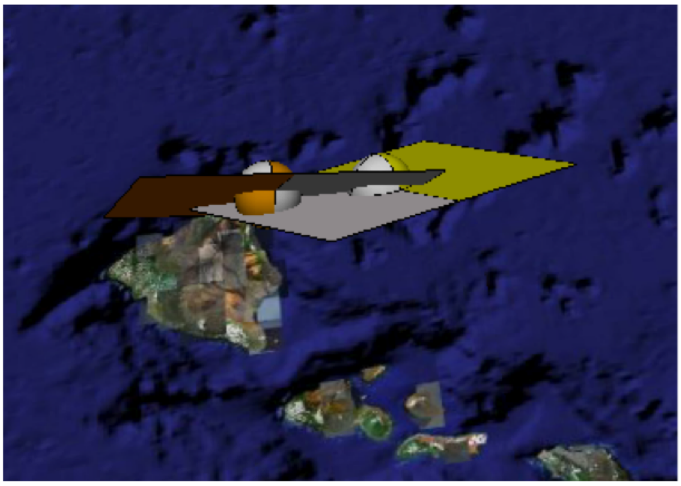

Another View of the same data from the Kiholo Bay event, Hawaii, 2006 (data from USGS NEIC and Havard/LDEO)

Figure 9c. Fault plane versus auxiliary plane

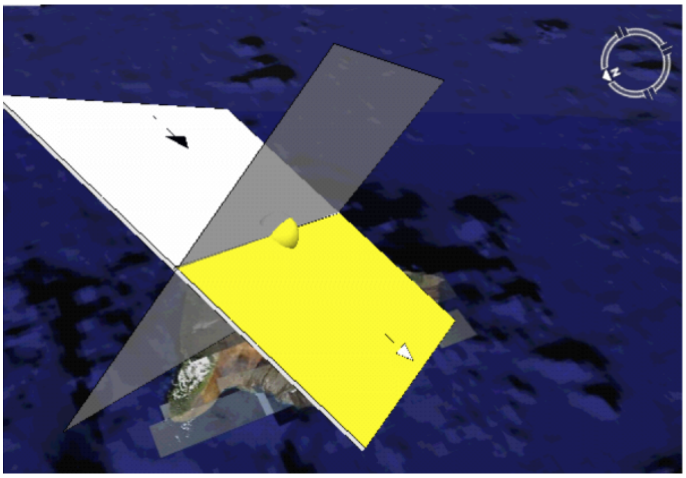

Solid models for the fault plane (arrows indicate sense of double-couple shear) and the auxiliary plane (semi-transparent). Beach ball is visible at center.

The planes are colored where they bound contractional first motions (T quadrants) and are white where adjacent to dilatational (P) quadrants of the associated beach balls. Default versions of the models are included in the download file with the file names such as NP_Black. dae, NP_Blue.dae, *etc.* Variants with small arrows marking fault slip directions are labeled NParo_Black.dae, NParo_Blue.dae, *etc.*

The example illustrated in Figure 9 represents two different focal mechanism solutions for the 2006 Kiholo Bay earthquake. The same approach could be taken to representing aftershocks and neighboring historic events. In Figure 10, multiple nodal planes for historic earthquakes in the Hawaiian eastern rift zone reveal the presence of a low angle décollement surface. Click here for a movie version of this image [Kiholo Bay movie]

Figure 10. Hawaiian historic data

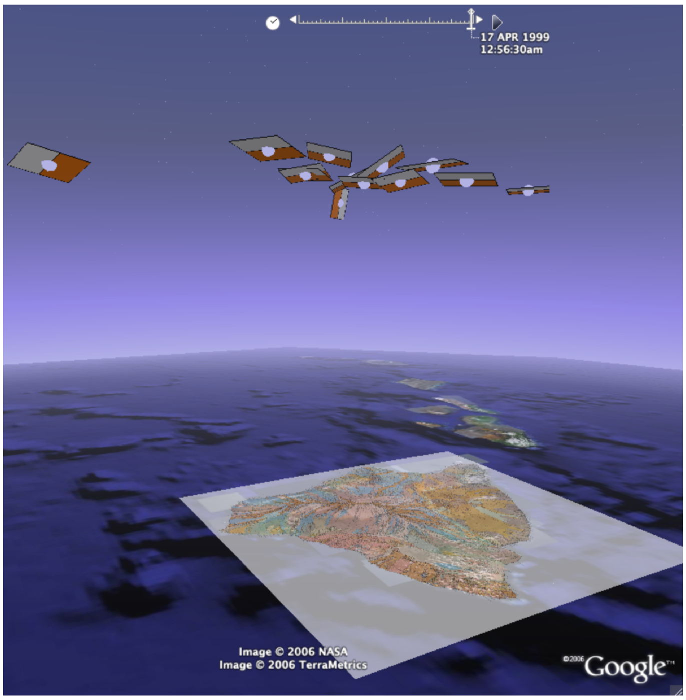

Nodal plane solid models for historic earthquakes (1970 - present, as reported by the USGS NEIC) in the eastern rift zone of Hawaii's main island reveal the presence of a gently northwest-dipping décollement. Foci are bumped out by 50 km.

Representing non-double-couple centroid moment tensors

The full centroid moment tensor solution for an earthquake (the so-called Harvard/LDEO CMT) may include a non-double-couple element, especially where seismicity is associated with magmatism, hydrothermal activity, or landslip (Jullian *et al.* 1998, Miller *et al.* 1998, Yunga *et al.* 2005). The solution is then represented graphically (Figure 11a) by the intersection of the moment tensor's eigen-ellipsoid with a concentric focal sphere.

Figure 11a. Basketball models

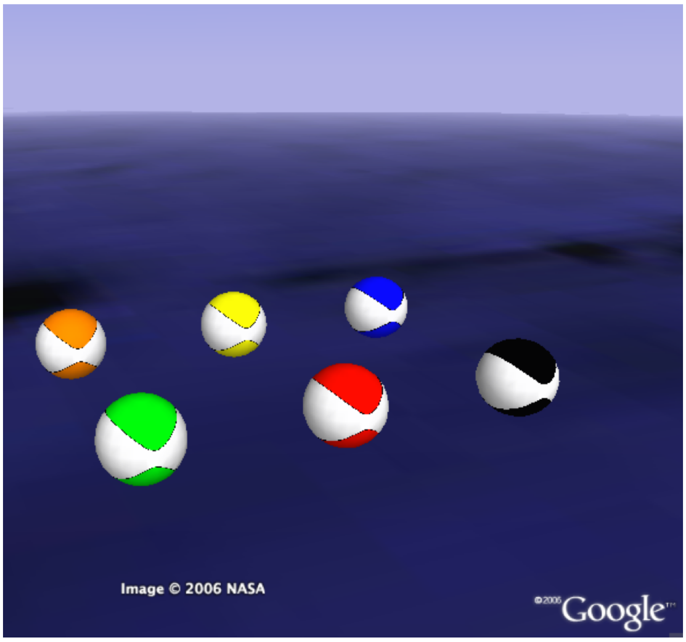

Non double couple Centroid Moment Tensor (CMT) solution yields a "basket ball" model. Model created by intersecting a bi-cone of elliptical base with a concentric sphere.

Figure 11b. Pool ball model

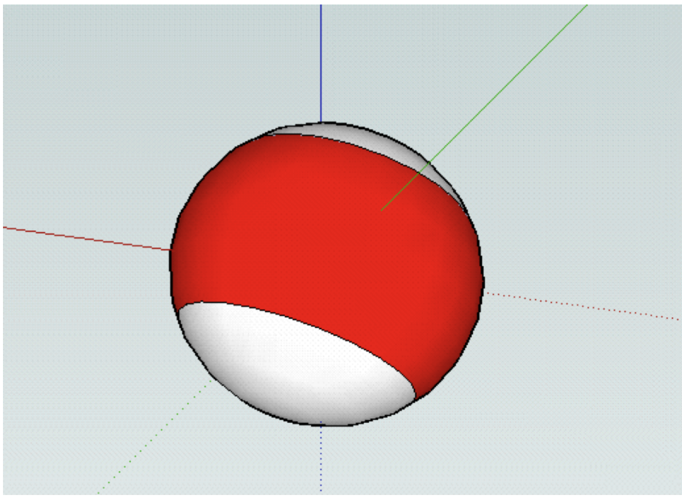

Special case of a CMT with a spheroidal eigen-ellipsoid yields a small circle ("pool ball") model. This model is generated by intersecting a sphere with a bi-cone of circular base.

Figure 11c. CMT eigen-ellipsoid

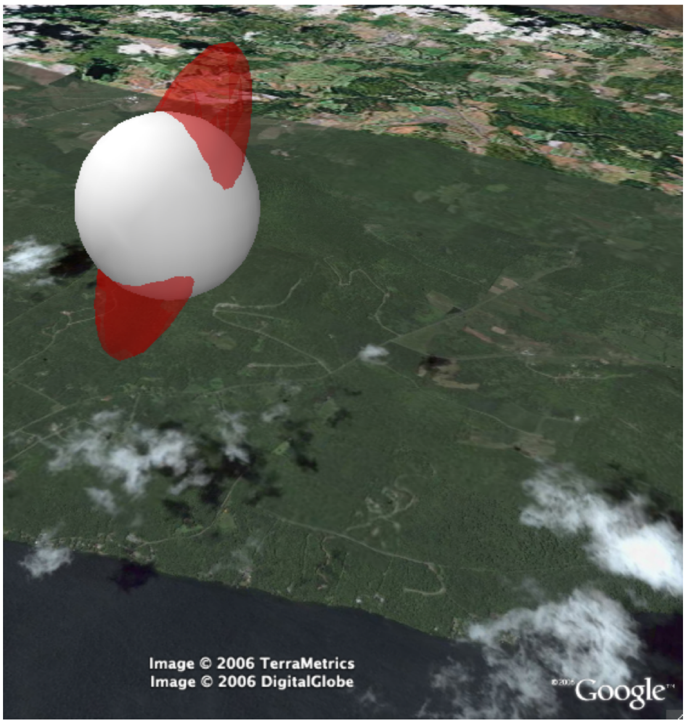

Alternative representation of CMT components using intersecting semi-opaque sphere and moment tensor eigen-ellipsoid. This sample does not represent a real event.

This line of intersection is a spherical ellipse and it defines a bi-cone of elliptical base – a non-planar nodal surface that separates directions of contractional and dilatational first motions just as the pair of nodal planes did in simple double-couple movements. The diagram may be thought of as a geophysical basketball. However, in special cases of spheroidal eigen-ellipsoids, the semi-major and semi-minor arcs of the spherical ellipse are equal, the cone has a circular base, and the diagram looks more like a geophysical pool ball (Figure 11b). A range of sample non-DC CMT solutions are available from the download file. For precise dimensions, it is most efficient to use the representation in Figure 11c which is created by superimposing a semi-opaque sphere and ellipsoid concentrically. Note in passing that a similar approach is ideal for representation of stress and finite strain data in 3 dimensions (De Paor & Pinan-Llamas 2006).

Relating nodal planes and surfaces to first arrivals

While experimenting with solid models of nodal planes and biconic surfaces, the author discover the truly remarkable capacity of Google Earth to represent very large objects. Figure 12a shows two nodal planes with <x> <y> <z> scale tags (Table 4) set to extend across the diameter of the Earth. The planes slice the Earth into regions of compressional ("up") and dilatational ("down") first arrivals. These models are extremely useful for pedagogy as they relates the zones of distinct first arrivals to the orientation of the focal mechanism diagram, and they may also have research applications in checking on the consistency of regional geoseismic data, especially for complex cases of non-double-couple solutions (Figure 12b). Click here for a movie version [Nodal planes movie]

Figure 12a. Global scale nodal planes

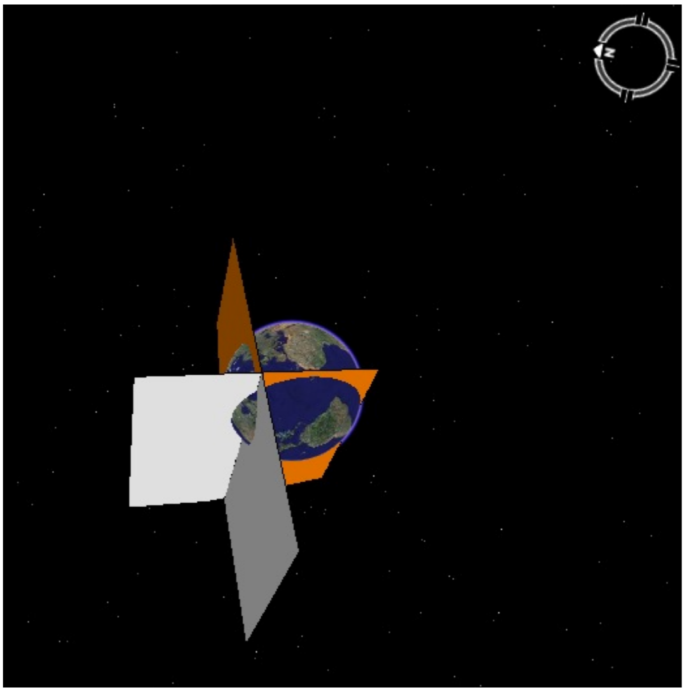

Nodal plane solid models are here magnified to a global scale. Beach ball lies at the center of the line of intersection of the nodal planes but is not visible in this view. This visualization is extremely useful for illustrating the relationship between the quadrants of the geophysical beach ball (not visible in this view) and the regions of the earth surface that record "up" versus "down" first motions.

Figure 12b. Global scale nodal surface

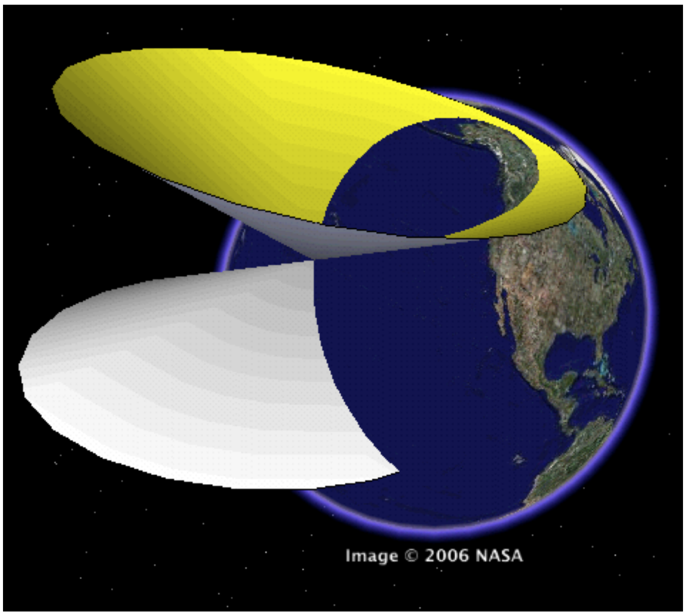

Bi-cone solid model of non-DC nodal surface here magnified to a global scale. This visualization is useful for illustrating the relationship between the regions of the geophysical basket ball (at apex – not visible) that receive distinct first motions.

Event times and timespans

Version 4.0 of KML introduced tags that enable data to be introduced to the Google Earth virtual globe in a temporal sequence. Table 6 shows the basic syntax.

Table 6: Timespan Tags for Sequences of Events in Google Earth

```
<Placemark>
    <TimeSpan>
        <begin>1979-09-22T07:50:42Z</begin>
        <end>1979-09-22T07:55:42Z</end>
    </TimeSpan>
    <Model>...
    </Model>
</Placemark>
```

Most geophysical applications will involve only an event start time, in which case the <end> tags are omitted. The time format follows standard XML protocols (*www.w3.org*). Click here for a quicktime movie from De Paor & Williams 2006 [AfterShocks movie] and here for an example from De Paor and Pinan-Llamas 2006 [Andes Timespan movie]

Figure 13. Hawaiian aftershock sequence

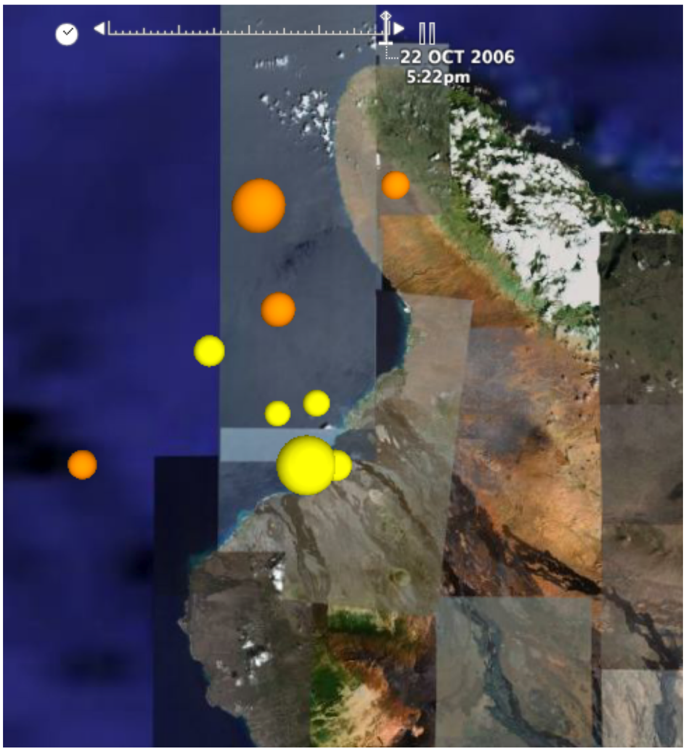

Timespan tags enable seismic events to be added to the Google Earth terrain in their correct temporal sequence. Here aftershocks are represented by solid spheres because focal mechanism solutions are not available.

Figure 13 is a still screen shot from a Google Earth timespan showing the sequence of aftershocks for the Kiholo Bay earthquake. Here, the times on the time controller are real dates. However, there are many geophysical and geological applications in which a pre-historic time line would be essential. Experimentation shows that timespan tags accept small negative dates, however, bugs occur when dates exceed a few thousand years, and the program hangs if a start date of negative 4,500 million years is used. At present, the only solution is to scale down the timescale, for example, to let a timespan of 4,500 years, represent the 4.5 b.y. geological record or a timespan of 543 years represent the Phanerozoic.

Real-time monitoring

KML tags permit network links to remote data servers. The example shown in Table 7 links to a USGS server and allows the user to view earthquakes in near-real time on their Google Earth virtual globe.

Table 7: Network Link Tags for Access to Remote Data

```
<NetworkLink>
  <name>Earthquakes</name>
    <Url>
      <href>http://earthquake.usgs.gov/eqcenter/catalog
      <refreshMode>onInterval</refreshMode>
      <refreshInterval>300</refreshInterval>
    </Url>
 </NetworkLink>
```

The refresh mode and refresh interval tags control the way in which the display is kept up to date. Currently, there are no KML sources for focal mechanisms and centroid moment tensor solutions. The author has successfully parsed HTML documents such as those on the USGS NEIC serve, searching for key words (“NP1”, “NP2”, “strike”, “dip”, “slip”) and reading the digits that follow. However, this is an unsatisfactory “hack”-like solution as it is easily broken by a change in HTML page source format. The USGS currently issues email alerts with nodal plane solutions so it should be possible to post the same data in KML format. KML based nodal plane data may thus be expected in the near future.

Shake maps and community feedback

THE USGS currently invites community feedback in the form of “Did you feel it” questionnaires. Given the ubiquitous availability of camera-cell phones, it should be possible to invite community contributions of geo-referenced damage photographs for inclusion in Google Earth tours. De Paor & Williams (2006) created such a tour manually (Figure 14).

Figure 14. Hawaiian damage report

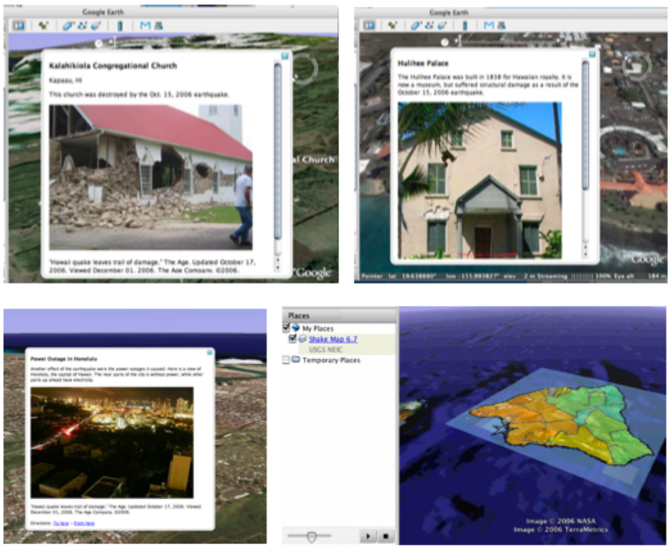

De Paor & Williams (2006) included damage reports and images in Google Earth placemarks, making it easy to view damage in relation to shake maps and moment tensor solutions.

Damage reports and images were placed in Google Earth place marks and a shake map was overlain on the terrain using KML <groundoverlay> tags. The resultant KML file permits theoretical analyses such as focal mechanisms and centroid moment tensors to be viewed in conjunction with damage data. Such analyses may improve future forecasts and analyses of earthquake hazards.

Conclusions

The Sumatra-Andaman tsunami of December 2004 heightened public awareness of the potentially devastating scale of such infrequent natural disasters. An earthquake will generate a tsunami if and only if it possesses a threshold magnitude, an appropriate geographic location, and particular focal mechanism geometry. The Hawaiian Kiholo Bay earthquake of 2006 did not produce a dangerous tsunami, but it demonstrated that so-called aftershocks can be almost as large as the main event. It is therefore useful to have access to timely data! Modern desktop and laptop computers, and even video cell phones, and other pocket devices (PDAs) are capable of displaying seismic data in real time and can be programmed to receive alerts. Timely communication of hazards (e.g., Hirshorn 2006) may benefit from delivery of data in easily comprehended format directly to the vulnerable population rather than indirectly via public officials, some of whom are bound to be on their cigarette break, or otherwise inattentive, at the crucial moment. The use of virtual globe technologies such as Google Earth and NASA World Wind hold great promise for enhancing the ability of the public and experts alike to visualize, analyze, and evaluate natural hazards.

Acknowledgments

The author acknowledges support from the National Science Foundation, NSF EAR 0310232: “Real-time Monitoring, Enhanced Visualization and Temporal Analysis of Tectonic and Geophysical Data.” The work benefited from discussions and interaction with students Heather Melanson, Liz Wilson, Arancha Pinan, Liam Morley, Nathan Williams, and Akanksha Sharma.

References

Babaie, H.A., and Babaei, A., 2002. SGeoML, An XML markup language for communication and processing of structural geological information. Geological Society of America Abstracts with Program, v. 34, (6), p.374

Cronin, V., 2004. A Draft Primer on Focal Mechanism Solutions for Geologists. http:// serc.carleton.edu /files/ NAGTWorkshops / structure04 /Focal_mechanism_primer.pdf (Vince_Cronin@baylor.edu)

De Paor, D.G., 1999. Tectonic Markup Language - An Idea Whose Time has Come. Geological Society of America Annual Meeting, Philadelphia, #52062. http://rock.geosociety.org/absindex/annual/1999/52062.htm

De Paor, D.G., Wilson, E. and Melanson, H. 2006. A Focal Mechanism Diagram Generator for Analysis of Earthquake First Motions. In: (eds.) Köhn, D. and De Paor, D., General Contributions, Journal of the Virtual Explorer, electronic edition, vol. 22. http://users.wpi.edu/~declan/

De Paor, D.G. and Pinan-Llamas, A. 2006. Application of Novel Presentation Techniques to a Structural and Metamprhic Map of the Pampean Orogenic Belt, NW Argentina. Geological Society of America Annual Meeting, Philadelphia, 38 (7): p.326. #131-12. http://gsa.confex.com/gsa/2006AM/finalprogram/abstract_112392.htm

De Paor, D.G. and Williams, N.R., 2006. Solid Modeling of Moment Tensor Solutions and Temporal Aftershock Sequences for the Kiholo Bay Earthquake Using Google Earth With a Surface Bump-out. EOS Transactions of the American Geophysical Union, Fall Meeting, San Francisco, Abstract S53E–05

Hirshorn, B. F. 2006. The Pacific Tsunami Warning Center Response to the MW6.7 Kiholo Bay Earthquake. EOS Transactions of the American Geophysical Union, Fall Meeting, San Francisco, Abstract S53E-02

Hogan, P. and Kim, R. 2004. NASA Planetary Visualization Tool. EOS Transactions of the American Geophysical Union, Fall Meeting, San Francisco, Abstract SF13A-0701

Hogan, P. and Kuehnel, F. 2006. NASA World Wind, Open Source 4D Geospatial Visualization Platform: *.NET & Java* for Education. EOS Transactions of the American Geophysical Union, Fall Meeting, San Francisco, Abstract ED23C-02

Julian, B. R., Miller, A. D., and Foulger, G. R. 1998. Non-double-couple earthquakes, 1, Theory, Reviews of Geophysics, v. 36 (4): 524-549 10.1029/98RG00716

Lisa, M., Khan, S.A., and Khwaja, A.A., 2004. Focal mechanism study of north Potwar de-formed zone, Pakistan. Acta Seismologica Sinica, v. 17, No.3 (255~261) Article ID: 1000-9116(2004)03-0255-07. http:// www.cea-igp.ac.cn / English.files /ass /ass2004 /ASS_2004_3_Mona.pdf

McNutt S. R., and Sánchez, J. J., 2000. Composite Focal Mechanisms at Four Alaskan Volcanoes. 95th annual meeting of the Seismological Society of America, 9-12 April 2000, San Diego, CA, USA

Miller, A. D., Foulger, G. R., and Julian, B. R. 1998. Non-double couple earthquakes 2. Observations. Reviews of Geophysics v. 36 (4): 551 - 568 10.1029/98RG00717

Scholz, C. H. 2002. The Mechanics of Earthquakes and Faulting, 2nd ed. Cambridge University Press, 471pp. ISBN 0521655404

Stein, S. and Wysession, M. 2002. Introduction to Seismology, Earthquakes, and Earth Structure. Blackwell Publishing, 512pp. ISBN 0865420785

Yunga, S., Lutikov, A., and Molchanov, O. 2005. Non double couple seismic sources, faults interaction and hypothesis of self-organized criticality. Natural Hazards and Earth System Sciences v. 5: 11-15.